Dye-concentrated organically modified silica nanoparticles as a ratiometric fluorescent pH probe by one- and two-photon excitation†

Sehoon Kim, Haridas E. Pudavar and Paras N. Prasad*

Received (in Cambridge, UK) 23rd January 2006, Accepted 23rd March 2006
First published as an Advance Article on the web 6th April 2006
DOI: 10.1039/b600926c

Basic dye-concentrated nanoparticles (~ 33 nm in diameter) show fluorescence-based ratiometric pH response, by one- and two-photon excitations, with improved proton sensing ability (pK_a ~ 6.4) through nanoscopic intraparticle energy transfer.

Growing demands on pH monitoring for environmental, biomedical, and bioprocess applications have driven the development of fluorescence-based techniques in recent years, due to many advantages which include greater sensitivity and ease of miniaturization, *etc*. This technique also benefits from the availability of various natural and synthetic fluorescent probe molecules.[1,2] In particular, fluorescent indicators that exhibit pH-driven wavelength alterations in their emission spectra allow for a more reliable detection in a dual-emission ratiometric manner, which eliminates data distortions caused by instrumental instability, photobleaching, and probe concentration.[2,3] However, most current pH indicators display response only in fluorescent intensity, with the exception of a few available probes including HPTS (8-hydroxypyrene-1,3,6-trisulfonic acid), SNAFL (seminaphthofluoresceins) and SNARF (seminaphthorhodafluors).[1–3] Consequently, the development of tailor-made ratiometric probes, by matching the pK_a to the pH of the experimental system, is gaining great interest for better performances in various pH ranges of interest, for example in intracellular monitoring, pH 6.8–7.4 in the cytosol and 4.5–6.0 in the cell's acidic organelles.[2,4] In cellular research, nanosensors based on PEBBLEs (probes encapsulated by biologically localized embedding) have been investigated due to many advantages over free dyes, such as biocompatibility and nontoxicity, *etc*.[5]

In this paper, we propose the novel concept of a nanoparticle-based fluorescent pH indicator for near-physiological use. The designed particulate indicator is characterized by nano-assembly of a pH-probing hydrophobic molecule, *i.e.*, organically modified silica (ORMOSIL) nanoparticle which is concentrated with a ratiometric pH-responsive organic dye. ORMOSIL nanoparticles are known as a water-dispersible and biocompatible carrier for hydrophobic dyes in aqueous media.[6] As for the hydrophobic dye, we chose a naphthalenylvinylpyridine derivative (NVP, see Scheme 1), where the pyridyl unit is a proton receptor. Like other pyridine-based dyes,[7] NVP responds to proton, with fluorescence red-shift from high-energy blue to low-energy yellow. In the NVP-concentrated ORMOSIL nanoparticle, it is expected that the dyes would be densely dispersed everywhere through the nanoparticle, where the proton-sensing event will take place mainly near the surface. Given this localized event, the high-energy neutral and the low-energy protonated states will closely coexist in the inner and the surface parts of the nanoparticle, respectively, enabling the inner-to-surface energy transfer. By virtue of such construction in nano-space, the proton sensitivity, in terms of fluorescence, would be improved by the energy transfer which amplifies the energy-accepting protonated surface signal, and thus the apparent pK_a value of the nanoparticle will be modified from that of the dye component. Pyridine-based dyes have potential for large two-photon activity.[8] Nevertheless, their use in pH probing, in general, is restricted to rather acidic environments, as they are less sensitive to protons, due to low pK_a values.[2,7] Thus, our strategy offers an easy way to increase their low pK_a values to a physiological level. We report the preparation of NVP-concentrated ORMOSIL nanoparticles and their intraparticle energy transfer characteristics. Also demonstrated is the ratiometric pH-sensing behavior in the near-physiological range, based on fluorescence emission by one- and two-photon excitations.

Synthetic procedures for NVP and its ORMOSIL nanoparticle (OSNP) are depicted in Scheme 1. NVP was obtained exclusively in a *trans*-form by Heck coupling between bromonaphthalene (**1**) and 4-vinylpyridine. To achieve a large loading amount without leak-out, NVP was functionalized into a silicate precursor (Si-NVP) to be attached chemically to OSNP, by using 2-fold

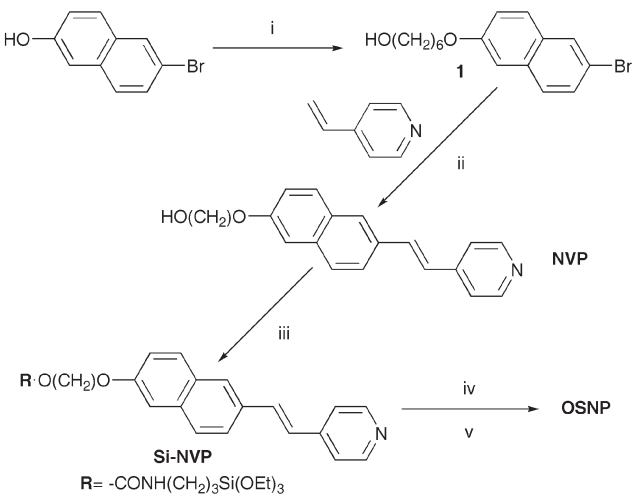

Scheme 1 *Reagents and conditions*: i) $HO(CH_2)_6Cl$, K_2CO_3, KI, 18-crown-6, DMF, 30 °C. ii) $Pd(OAc)_2$, P(*o*-tolyl)$_3$, Et_3N, THF, 80 °C. iii) 2-fold ICTES, Et_3N, dibutyltin diacetate, THF, reflux. iv) Hydrolysis, NH_4OH, THF, room temperature. v) Assembly into nanoparticle and sol-gel condensation in aqueous micelle of AOT/1-butanol, room temperature.

Institute for Lasers, Photonics and Biophotonics, Department of Chemistry, State University of New York, Buffalo, New York, 14260-3000, USA. E-mail: pnprasad@buffalo.edu

† Electronic supplementary information (ESI) available: Experimental details, one-photon absorption, fluorescence, and excitation spectra of NVP monomer and OSNP. See DOI: 10.1039/b600926c

equimolar (3-isocyanatopropyl)triethoxysilane (ICTES). After complete reaction, as determined by thin layer chromatography, the resulting mixture was used for the next steps without purification. The remaining excess ICTES acts as a co-monomer for sol-gel polymerization, which possibly hinders close packing of the NVP chromophores in the concentrated nanoparticle, to minimize the intermolecular fluorescence quenching effect. OSNP was obtained by sol-gel condensation in an aqueous micellar medium of sodium bis(2-ethylhexyl)sulfosuccinate (AOT) and 1-butanol. After removal of surfactants by dialysis against water, stable aqueous dispersions of OSNP were obtained with the help of hydrophilic surface silanol groups.

One- and two-photon optical properties of the NVP monomer were examined in aqueous solution (Fig. 1a–b). A mixed solvent, DMSO/water (= 1/1 by volume), was used to ensure homogeneous dissolution in the micro-molar concentration range since the NVP monomer is hydrophobic and not soluble in water. Fig. 1a shows the optical responses of the NVP monomer to a change from neutral to acidic or basic conditions. Upon acidification, absorption and fluorescence spectra are shifted to a longer wavelength by protonation, due to the increased intramolecular charge transfer (ICT) character. The fluorescence quantum yields (Φ_f) in the neutral blue and the protonated yellow states were estimated as 0.06 and 0.18, respectively. Upon basification, absorption change is negligible, while fluorescence exhibits a slight decrease in intensity at the longer wavelength tail. The excitation spectra for the tail emission at 600 nm, near the peak of the protonated emission, show a noticeable change, where the protonated band at *ca.* 400 nm was observed even in neutral conditions but was depressed by basification (Fig. S1 in ESI†). Note that the actual pK_a value of NVP is not obtainable, owing to its water insolubility. However, the above optical changes indicate that the population of the protonated state under neutral conditions is so low as to be slightly detected only by its three-fold more efficient emission, suggesting its low pK_a value.

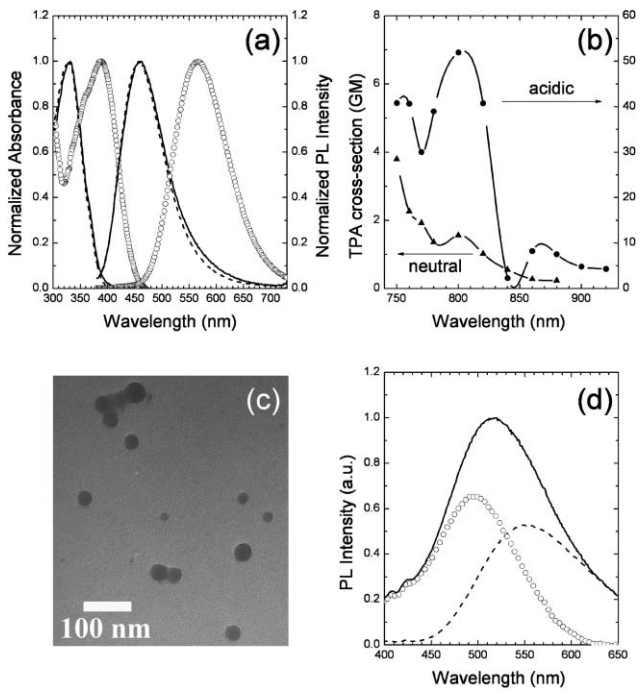

Fig. 1 (a) Normalized one-photon absorption and photoluminescence (PL, excited at 370 nm) spectra of NVP in neutral (solid line), basic (dashed line), and acidic (circle) conditions. (b) Two-photon excitation spectra of NVP in neutral (triangle) and acidic (circle) conditions. 1 GM = 10^{-50} cm^{4}s(photon-molecule)$^{-1}$. (c) TEM image of the obtained OSNP. (d) Peak separation of the OSNP emission at pH 7 (solid line) into the neutral (circle) and the protonated (dashed line) components.

It is also noteworthy that in Fig. 1a the red-shifted absorption by protonation partially overlaps with the shorter-wavelength side of the neutral blue emission. One can anticipate Förster-type energy transfer from the neutral to the protonated NVPs, if the two states exist in proximity, as in the case of OSNP. In solution, however, such intermolecular interaction was not observed, when examined with the partially protonated solution, by a certain amount of citric acid, containing both neutral and protonated NVP (Fig. S2 in ESI†). Since they are separated with each other by solvation, the neutral and the protonated NVP contribute independently to dual emission at 460 and 565 nm, respectively, in a typical ratiometric manner. This independent behavior in solution is no more the case for the NVP-concentrated OSNP, where the emission spectrum is changed by nanoscopic intraparticle energy transfer (*vide infra*).

The TPA cross-sections (σ_2) of the NVP solution in neutral and acidic conditions were measured by the two-photon-induced fluorescence method,[9] using a femtosecond Ti-sapphire laser (Fig. 1b). In the spectral window of 750–920 nm, the maximum two-photon absorptivity in the neutral and the acidic conditions is 4 GM at 750 nm and 52 GM at 800 nm, respectively, where the large enhancement for the latter is due to the increase in ICT character. These values are comparable with those of commonly used fluorescent probes such as fluoresceins and rhodamines,[9] enabling two-photon application of the NVP-concentrated OSNP.

The spherically shaped OSNP with a diameter of 33 $\pm$ 6 nm was successfully obtained in the micellar medium, as shown by the transmission electron microscopic (TEM) image in Fig. 1c. In neutral water, the OSNP dispersion exhibits the neutral NVP-like absorption at 332 nm, with the baseline offset by Mie scattering, while its fluorescence is positioned at 513 nm, between those of the neutral and the protonated NVP monomers (Fig. 1d and Fig. S3 in ESI†). These optical properties of OSNP were maintained even after 6 months of storage in the dark and were observed to be stable during the measurements without any sign of photodegradation. Moreover, they are maintained even in an NVP-solubilizing mixed solvent, DMSO/water (= 1/1 by volume), supporting the formation of a rigid chemical construction within the nanostructure (Fig. S3 in ESI†). The similarity of fluorescence quantum yields between OSNP and NVP in the neutral mixed solvent (Φ_f = 0.04 and 0.06, respectively) implies that the excess co-monomer, ICTES, is effectively minimizing the intermolecular quenching process in the concentrated nanoparticle.

The unusually symmetric OSNP emission spectrum at pH 7 seems to be a mixed one, and thus can be analyzed into two peaks derived from the neutral and the protonated contributions. This is because, as mentioned above in relation to Fig. 1a, a certain amount of the protonated NVP exists already even in neutral conditions, undoubtedly on the surface in the case of OSNP. Fig. 1d shows the result of peak separation using the spectral shape of the OSNP emission at pH 4 for the longer-wavelength protonated component. The calculated shorter-wavelength neutral component at 494 nm is red-shifted with respect to the neutral

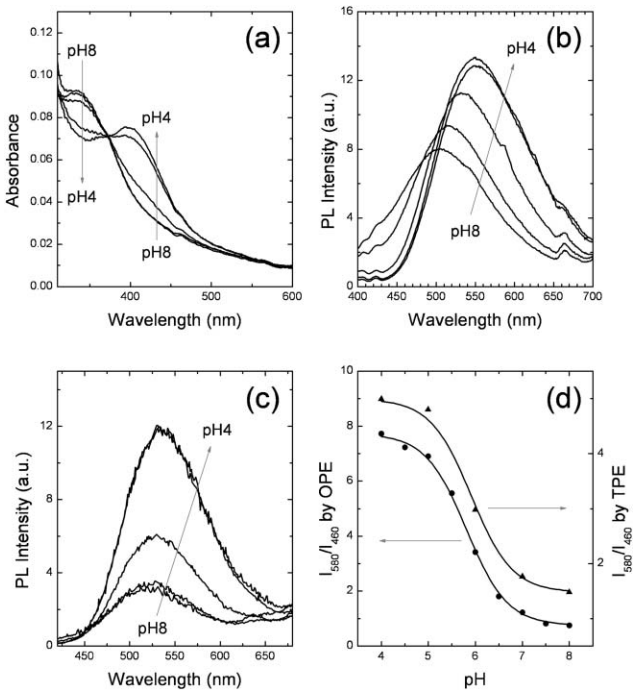

Fig. 2 pH-dependent spectral evolution of the OSNP dispersion: one-photon absorption (a) and PL (b, excited at 370 nm), and two-photon excited PL (c, excited at 780 nm). (d) Ratiometric plots of fluorescence intensities at 580 and 460 nm by one- (circle, excited at 370 nm) and two- (triangle, excited at 780 nm) photon excitations. The solid lines are the fitting results for experimental data by using Eqn. (1) in ESI†.

NVP monomer emission at 460 nm, suggesting the occurrence of energy transfer within OSNP. It is noted that, due to a partial overlap in Fig. 1a, only the shorter-wavelength side of the neutral NVP emission is transferred to the protonated one and the longer-wavelength energy is left, resulting in a red shift of the neutral component. Moreover, by virtue of energy transfer, the emission from the protonated NVP on the surface, in spite of there being a minimal amount, exhibits amplified intensity, comparable to the excess neutral component, validating our nanoparticle-based design strategy for improving proton sensitivity. The similarity in the excitation spectra below 400 nm for both emission components (at 450 and 600 nm, respectively) is evidence of intraparticle energy transfer, indicating protonated emission generated by neutral excitation (Fig. S4 in ESI†). Overall, the NVP-concentrated OSNP emits greenish mixed fluorescence even under neutral conditions, between the neutral blue and the protonated yellow ones of the NVP monomer.

The spectral evolution and the ratiometric behavior of OSNP under one- and two-photon excitation are shown in Fig. 2. The absorption and the emission spectra of OSNP show practically instantaneous responses to the pH change. The pH-dependence of the one-photon absorption in Fig. 2a displays a dual-absorption behavior, typical of ratiometric probes, with an isosbestic point at *ca.* 370 nm, indicating the ground-state conversion from neutral to protonated species. Upon excitation at 370 nm, however, OSNP emits no normal dual emission, but broad, single-peak fluorescence at every experimental pH, which becomes narrower and red-shifted with decreasing pH. This unusual behavior, different from dual emission of the NVP monomer (Fig. S2 in ESI†), is attributed to the intraparticle energy transfer which combines donor–acceptor emissions apparently into a single peak, as discussed above. The two-photon excitation of OSNP at 780 nm also produces a similar fluorescence spectrum and pH-dependence, except that the peak position and the intensity are slightly different at every measured pH, due to the different two-photon absorptivity of the NVP component between the neutral and the protonated states. Despite a lack of noticeable dual emission, the spectral evolution of one- and two-photon fluorescence of OSNP enables ratiometric probing in the range of pH 4–8 at room temperature, as shown in Fig. 2d. The intensity ratio of emissions at 580 and 460 nm varies with pH, by one order of magnitude under one-photon excitation and 3.4 times under two-photon excitation. Importantly, OSNP, which includes a less proton-sensitive pyridine-based dye, shows a greater response in the weak acidic range by virtue of the improved proton sensitivity. From the fitting of the titration curves, the same pK_a values ($\sim$ 6.4) were extracted by both one- and two-photon excitation, which are similar to the values obtained by a carboxyfluorescein probe, often used for near-physiological pH measurement.[2]

In summary, the basic dye-concentrated nanoparticle structure has been shown to improve the proton sensing ability, in terms of fluorescence, through nanoscopic intraparticle energy transfer from the neutral inner part to the protonated surface. We anticipate that our approach, based on the dye-concentrated ORMOSIL nanoparticle, will provide a promising pathway to near-physiological intracellular pH monitoring, due to its advantages which include water dispersibility, biocompatibility, and appropriate pK_a, as well as two-photon activity. Further, the surface silanol groups of ORMOSIL nanoparticles can be modified for targeted delivery, without affecting the intrinsic properties of sensor molecules.

This work was supported in part by a DURINT grant from the Chemistry and Life Sciences Directorate of the Air Force Office of Scientific Research and in part by the Post-doctoral Fellowship Program of Korea Science & Engineering Foundation (KOSEF).

Notes and references

1 B. Valeur, *Molecular Fluorescence: Principles and Applications*, Wiley-VCH Verlag GmbH, Weinheim, 2001.
2 R. P. Haugland, *Handbook of Fluorescent Probes and Research Products*, Molecular Probes Inc., Eugene, 9th edn., 2002.
3 J. R. Lakowicz, *Principles of Fluorescence Spectroscopy*, Kluwer/Academic Plenum Publishers, New York, 2nd edn., 1997.
4 D. E. Metzler, *Biochemistry: The Chemical Reactions of Living Cells*, Harcourt Academic Press, San Diego, 2nd edn., 2001, vol. 1.
5 H. A. Clark, R. Kopelman, R. Tjalkens and M. A. Philbert, *Anal. Chem.*, 1999, **71**, 4837.
6 T. K. Jain, I. Roy, T. K. De and A. N. Maitra, *J. Am. Chem. Soc.*, 1998, **120**, 11092; M. Lal, L. Levy, K. S. Kim, G. S. He, X. Wang, Y. H. Min, S. Pakatchi and P. N. Prasad, *Chem. Mater.*, 2000, **12**, 2632; I. Roy, T. Y. Ohulchanskyy, H. E. Pudavar, E. J. Bergey, A. R. Oseroff, J. Morgan, T. J. Dougherty and P. N. Prasad, *J. Am. Chem. Soc.*, 2003, **125**, 7860; X. Zhao, R. P. Bagwe and W. Tan, *Adv. Mater.*, 2004, **16**, 173.
7 Z. Diwu, C.-S. Chen, C. Zhang, D. H. Klaubert and R. P. Haugland, *Chem. Biol.*, 1999, **6**, 411; S. Charier, O. Ruel, J.-B. Baudin, D. Alcor, J.-F. Allemand, A. Meglio and L. Jullien, *Angew. Chem., Int. Ed.*, 2004, **43**, 4785; J.-M. Kim, T.-E. Chang, J.-H. Kang, K. H. Park, D.-K. Han and K.-D. Ahn, *Angew. Chem., Int. Ed.*, 2000, **39**, 1780.
8 B. A. Reinhardt, L. L. Brott, S. J. Clarson, A. G. Dillard, J. C. Bhatt, R. Kannan, L. Yuan, G. S. He and P. N. Prasad, *Chem. Mater.*, 1998, **10**, 1863.
9 C. Xu and W. W. Webb, *J. Opt. Soc. Am. B*, 1996, **13**, 481; M. A. Albota, C. Xu and W. W. Webb, *Appl. Opt.*, 1998, **37**, 7352.